объединенный
институт
ядерных
исследований
дубна

E2-84-236

N.S.Amelin, V.S.Barashenkov, N.V.Slavin

RESONANCE PARTICLE PRODUCTION IN INELASTIC N-N AND Π-N INTERACTIONS

Submitted to "Acta Physica Polonica"

1984

Phenomenological expressions describing the differential single-particle inclusive cross-sections of nucleon and π-meson production at high energies have been obtained in papers[1-3]. Their analytical structure has been defined with regard to the known theoretical models, and numerical coefficients have been selected from experimental data. These expressions not only accumulate a great body of experimental data in a wide energy region T* from 10 up to several thousand GeV, but provide the possibility of calculating the integral characteristics of secondary particles to analyse the properties of the leading particles[4], etc. From these expressions one can obtain estimations for those regions of kinematic variables, where measurements are still not carried out, and (using the Monte-Carlo method) simulate individual acts of inelastic collisions[5]**. Expressions obtained in refs.[1-3] can also be applied for resonance particle production. At present this fact is particularly important, since the experimental information on resonance production is rather limited and analytical approximation expressions possess a considerable predicting value.

Later on we shall confine ourselves to investigation of the Δ-, ρ- and ω-resonances, being produced up to extremely high energies at large cross-sections and presented by the greatest amount of experimental data. The approximation expressions are also suitable for other types of resonances. However, because of the lack of experimental data, which can be used for determination of the coefficients, these expressions give only a roughly-qualitative results.

---

*Below we always use the centre-of-mass system and the following notation: $\sqrt{s}$ is the total energy of the colliding particles, $E = \mathcal{T} + M$ and $\mathcal{T}$ are, respectively, the total and kinetic energies of the secondary particle considered, $p_{\parallel}$ and $p_{\perp}$ are the longitudinal and transverse momenta of this particle, $x = 2p_{\parallel} s^{-1/2}$. T is the kinetic energy of the projectile in the laboratory system.

**Using these expressions one ought to take into consideration, that they are concerned with the total postdecay characteristics and are used at sufficiently large distance from the interaction point.

Table 1

Coefficients for "conserved" and "unconserved" resonance particle spectra, described by expression (1) at $|x| < 0.7$

	Reaction \ Coefficient	a	b	c	d	f	g	μ^2	u	v
$|x| < 0.7$	$pp \rightarrow \{\Delta^+, \Delta^0, \Delta^{++}\} \ldots$	0.04	22. I. 20.	0.	3.3	0.09	5.4	I.77	0.I	-I.
$x > -0.7$	$\pi^+ p \rightarrow \Delta^{++} \ldots$	0.3	0.I	-0.2	4.05	I.5	5.9	I.2	6.5	-0.5
$x > -0.7$	$\pi^- p \rightarrow \Delta^{++} \ldots$	0.I	4.6	0	4.4	0.07	5.I	I.4	3.2	-0.5
$x < 0.7$	$\pi p \rightarrow \{\rho_{corp}, \rho^0, \omega\} \ldots$	4.8	0.95 0.8 0.5	-0.04	5.4	0.25	I.0 0.7 0.I5	I.26	0.65 0.65 0.4	-0.025

Table 2

Coefficients for "conserved" and "unconserved" resonance particle spectra, described by expression (1) at $|x| \geq 0.7$

Equal for all reactions				$|x| \geqslant 0.7$		$x \leqslant -0.7$				$x \geqslant 0.7$					
				$pp \rightarrow \{\Delta^+, \Delta^0, \Delta^{++}\}$		$\pi^+ p \rightarrow \Delta^{++} \ldots$		$\pi^- p \rightarrow \Delta^{++} \ldots$		$\pi p \rightarrow \rho_{corp}$		$\pi p \rightarrow \rho^0 \ldots$		$\pi p \rightarrow \omega \ldots$	
A				24,5; I.2*)		94		38.2		5.8		4.35		2.6	
R				4		0.0I		0.26		0.7		0.7		0.85	
α				0.4		2.		2.		I.		I.		I.	
1	α_1	β_1	γ_1	G_1	R_1	G_1	R_1	G_1	R_1	G_1	R_1	G_1	R_1	G_1	R_1
I	0	0	I.5	0.4 0.4 0.6	-0.8 -0.8 -0.7	I.5	-0.3	0.I8	-0.9	0.6	-0.37	0.6	-0.3	0.68	-0.I
2	0	-0.5	0.85	0.003	-0.9	-	-	0.004	-0.75	0.00I	-0.7	0.00I	-0.67	0.00I	-0.62
3	0.5	-0.5	I.5	-	-	3.	0.4	8	4.6	4.	6.	4.	6.	4.	6.
4	0	-I	0.2	0.3**) - -	I.5**) - -	-	-	-	-	-	-	-	-	-	-

*) for $pp \rightarrow \Delta^0$

**) for $pp \rightarrow \Delta^+ \ldots$

Table 3

Coefficients for "unconserved" resonance particle spectra, described by expression (2)

Reaction / Coeffic.	$-1 < x < 1$		$x > 0$		$x < 0$
	$pp \to \rho^{o}_{+} \dots$	$\pi^{\pm}p \to \rho^{\mp} \dots$	$\pi^{+}p \to \Delta^{++} \dots$	$\pi^{-}p \to \Delta^{++}$	$\pi p \to \{\rho_{cons}, \rho^{o}, \omega\} \dots$
a	0.3	I.6	I.0	0.4	I.9(I,6*)
b	$s^{0.2}$	4.	3.	3.	3.
c	0.4I	0.	0.	-0.07	0.
d	0.75	I.I	4.I	5.4	I.I
f	0.43	-0.0I	-0.32	-0.37	-0.0I
g	-3.0	-3.0	-2.	-I.	-3.
h	$2s^{0.2}$	5.	8.	7.	5.

*) Coefficient for reaction $\pi p \to \omega \dots$

Table 4

The ratio of the average multiplicities of resonance particles and all charged particles $\langle n_R \rangle / \langle n_{ch} \rangle$ in p-p and π^--p collisions at energy T (%)

T, GeV	p-p		π^--p	
	Δ^{++}	ρ^{o}	Δ^{++}	ρ^{o}
10	1.3	1.8	1.5	5.5
10^2	1.6	2.6	1.4	5.4
10^3	1.0	4.3	0.9	5.3
$5 \cdot 10^3$	0.8	6.4	0.8	5.4

Table 5

Energy dependence of the multiplicities of resonances created in inelastic p-p and π^--p collisions $\langle n(\mathcal{T}) \rangle / \langle n_{tot} \rangle$, $\langle n(\mathcal{T}) \rangle$ -average multiplicity of resonance with energy greater than $\langle n_{tot} \rangle = \langle n(\mathcal{T} = 0) \rangle$. The initial energy T = 1000 GeV

$\mathcal{T}/\mathcal{T}_{max}$	p-p		π^--p		
	Δ^{++}	ρ^{o}	Δ^{++}	ρ^{o}	ρ^{-}_{cons}
0.2	0.961	0.114	0.791	0.332	0.356
0.7	0.633	0.00063	0.437	0.058	0.068

Fig.1. Average multiplicity of Δ^{++} and ρ^{o}-resonances in inelastic p-p and π^--p collisions. The curves are the results of calculations, the points correspond to experimental data [6-42].

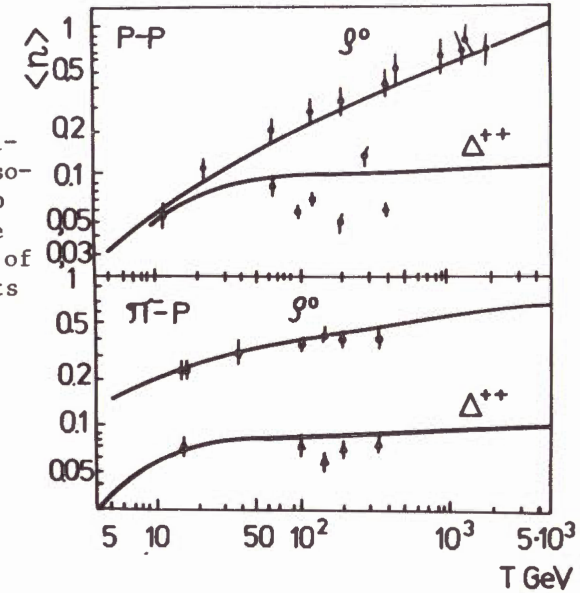

To describe the spectrum of "conserved"* particles we use the expression from paper [1]:

---

*We call the resonance particle R_a "conserved" in reaction $a + b \to R_a + \dots$ which is emitted in the forward hemisphere $(x > 0)$ and possesses the same quark composition as a primary particle a (for example, ρ^+ in reaction $\pi^+ + p \to \rho^+ \dots$), and also resonance R_b in reaction $a + b \to R_b + \dots$ which is emitted in the back hemisphere $(x < 0)$, and possesses the same quark composition, as a target b (Δ^+ p-p and π^+-p collisions).

$$E\frac{d^3\sigma}{d^3p}\left[\frac{mb}{GeV^2/c^3}\right]=\begin{cases} a(1+b|x|s^{c-x_\perp s^{0.27}})\dfrac{(1-|x|)^{fp_\perp^2}}{(p_\perp^2+\mu^2)^d}e^{g|x|}+us^v(1-|x|)e^{-5p_\perp^2}, & 0<|x|<0.7, \\ A|t|\dfrac{(1-|x|)^{1-\alpha t}}{(m_\pi^2-t)^2}e^{Rt}+\sum\limits_{i=1}^{4}G_i\left(\dfrac{s}{s_0}\right)^{-\alpha_i}(1-|x|)^{\beta_i-\gamma_i t}e^{R_i t} & 0{,}7\le|x|<1, \end{cases} \quad (1)$$

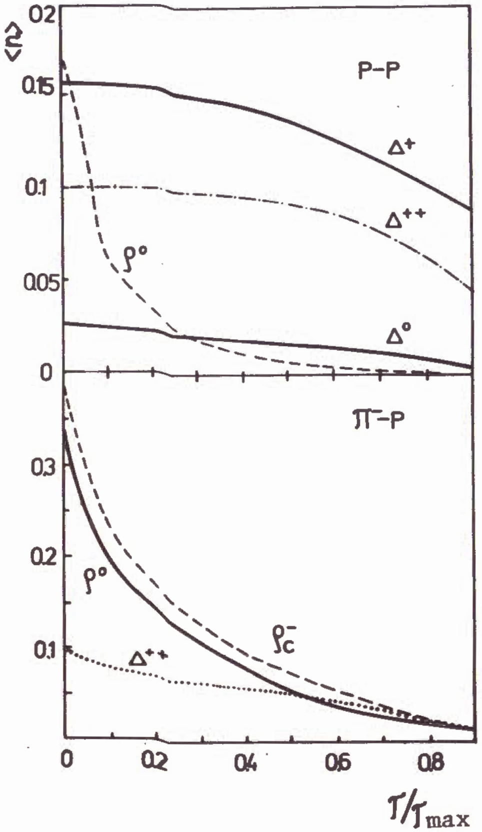

Fig.2. The average number of Δ- and ρ-resonances <n> with kinetic energies higher than $\mathcal{T}$. $\mathcal{T}_{max}$ is the highest possible energy of resonance particles. Inelastic p-p and π^--p interactions at T = = 100 GeV.

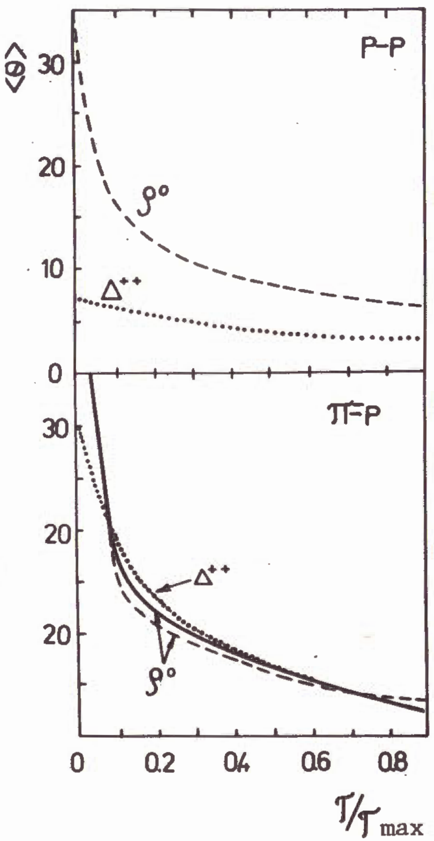

Fig.3. Average emission angle θ (in degrees) of Δ^{++}, and ρ°-mesons with kinetic energy higher than $\mathcal{T}$. Centre-of-mass system. Inelastic p-p and π^--p collisions at 100 GeV. In the case of π^--p interactions the values of ρ° for forward and backward hemisphere are plotted by solid and dashed curves, respectively.

where $t=-p_\perp^2/|x|-(1-|x|)(M_R^2/|x|-M_a^2)$. Here M_a and M_R are the particle masses in inclusive reaction $a+b\to R+X$, parameter s_0= 1 GeV^2, m_π is π-meson mass.

Expressions (1) can also be applied for description of R'_a and R'_b resonances in reaction $a+b\to R'_a(R'_b)+\ldots$ that differ only by one quark from a particle "a" (for example, Δ^{++} in reaction $pp\to\Delta^{++}\ldots$) and particle "b" (Δ^{++} in reaction $\pi^+ + p\to\Delta^{++}$ at $x<0$), accordingly.

Expression (1) can be also used for description of the spectra of ρ°- and ω-meson resonances produced in π-p interaction at $x>0$. The values of parameters for all these reactions are shown in Tables 1 and 2.

For the inclusive spectra of "unconserved" resonance particles (i.e., particles with a different from "a" and "b" particles quark composition, for example, ρ^+ in p-p and π^--p interactions) we use the same expression as in paper /2/:

$$E\frac{d^3\sigma}{d^3p}\left[\frac{mb}{GeV^2/c^3}\right]=a(1-|x|)^b\left[\frac{p_\perp^2 s^{c(1+|x|)}}{(p_\perp^2+1)^4}e^{-Rp_\perp^2}+\frac{ds^{f(1-|x|)}}{(|x|+1)^g}e^{-hp_\perp^2}\right], \quad /2/$$

where R = 0.75 $(GeV/c)^{-2}$ but values of coefficients b and h may depend on s. The values of parameters are shown in Table 3.

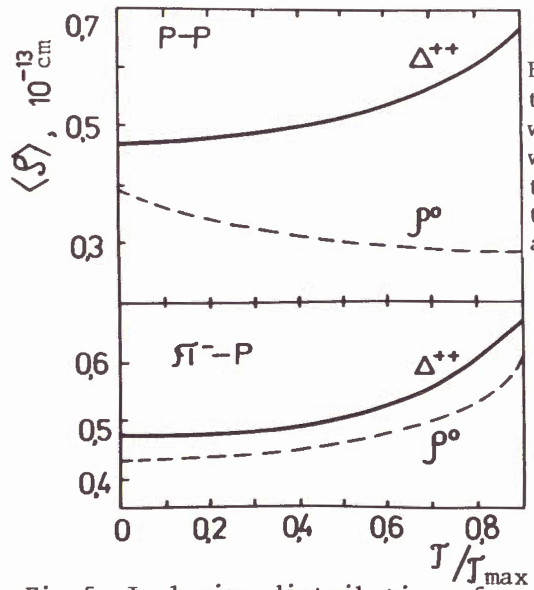

Fig.4. The distribution of the average distances at which the resonance particles with kinetic energies higher than $\mathcal{T}$ are produced. Inelastic p-p and π^--p interactions at 100 GeV.

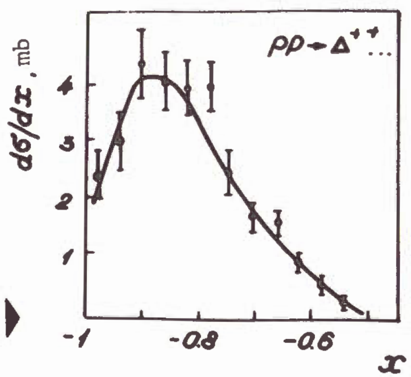

Fig.5. Inclusive distribution of dσ/dx for Δ^{++} resonances in p-p collisions at T = 68 GeV in the region |t| < 0.8 $(GeV/c)^2$ /7/.

Table 6

Meson resonance production cross-section in π^+p collision at 15 GeV

Particle / σ incl. (mb)	ρ^o	ρ^+	ρ^-	ω
experiment [36]	4.8±0.4	5.3±0.9	2.3±0.5	4.0±0.7
calculation	4.95	5.43	2.2	3.94

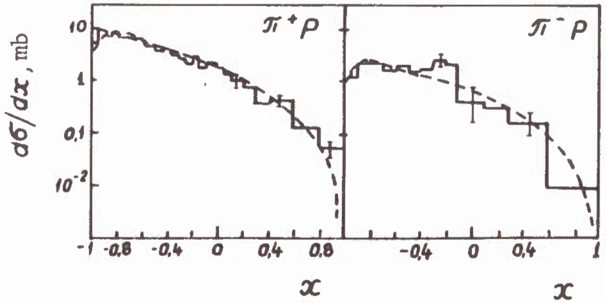

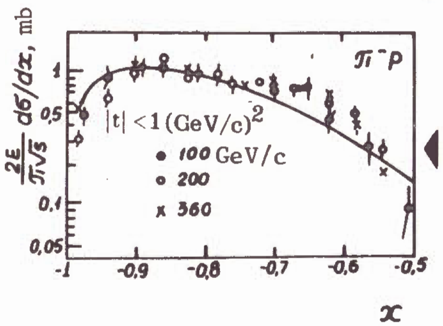

Fig.6. Distribution of $d\sigma/dx$ for Δ^{++} resonances in π^--p collisions at T = 15 GeV. The curves are the results of calculations; The histograms and experimental points in the region $|t| < 1\,(GeV/c)^2$ are taken from [8,41].

For the case of p–p interaction the coefficients for the ρ^o -meson only are presented in this Table. However, these coefficients can be used for approximation of inclusive cross-section of $\rho^{\pm}$ -mesons if one is restricted to the energy region about several dozens of GeV, since the experimental data show that ρ -meson spectra do not depend on the charge sign. The data at higher energies are not yet available.

As for ω -meson, available experimental data provide the possibility of defining the coefficients only for π-p interaction.

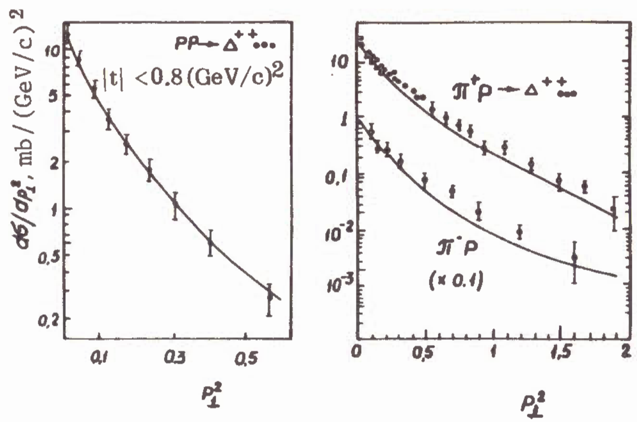

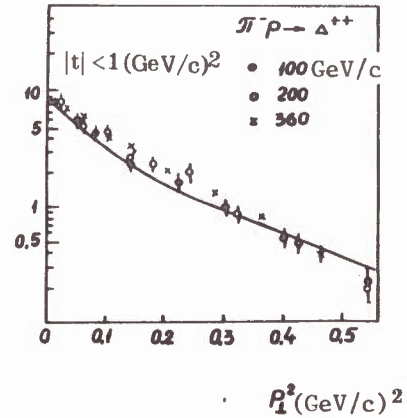

Fig.7. Distribution of $d\sigma/dp_\perp^2$ for Δ^{++} resonances in p–p collisions at T = 68 GeV and π^--p collisions at T = 15 and 100 GeV. Experimental points are taken from [7,8,41].

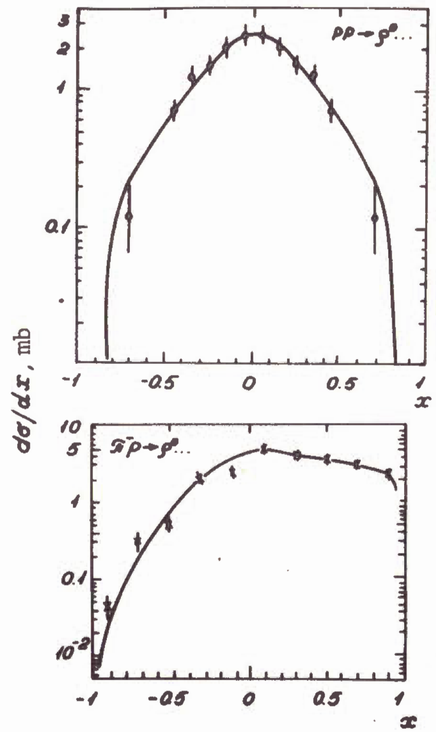

Fig.8. Distribution of $d\sigma/dx$ for ρ^o -mesons in p–p collisions at T = 11 GeV and π^--p collisions at 15 GeV. Experimental points are taken from [9–11].

Experimental data for Δ^+ and Δ^o-particles are still unsufficient. The absolute value of Δ^o-resonance production cross-section can be estimated from data in ref./7/. Proceeding from the identical quark composition of the Δ^+ and p, Δ^o and n, accordingly, the shape of the Δ^+ spectra can be chosen approximately the same as for proton spectra; and the shape of the Δ^o-spectra, the same as for neutron. The corresponding coefficients are presented in Tables 1 and 2. In Fig.1 the average multiplicities of Δ^{++}- and ρ^o-resonances calculated by expressions (1) and (2) are compared with experiment. Within the accuracy of the experimental data available at present a good agreement is achieved for the region of $T > 10$ GeV. As the primary particle energy increases, the average multiplicity of the Δ^{++}-resonance rises something slower than the total multiplicity of charged particles $\langle n_{ch}\rangle$ (Table 4). The multiplicity of ρ^o-meson in π^--p collision behaves similarly. At the same time in the proton collisions the number of produced ρ^o-mesons increases more rapidly than $\langle n_{ch}\rangle$.

Agreement of the calculated and experimental ρ^+-and ω production cross-sections is illustrated by Table 5. In the region of several dozens of GeV, where the coefficients of the approximation expressions are being selected, the agreement is satisfactory. At greater energies, where the experimental data are not available, the calculated values are considered only to be roughly-qualitative.

Table 6 and Fig.2 show the quantities of the resonance Δ-, ρ-particles with kinetic energy higher than $\mathcal{T}$ produced in ine-

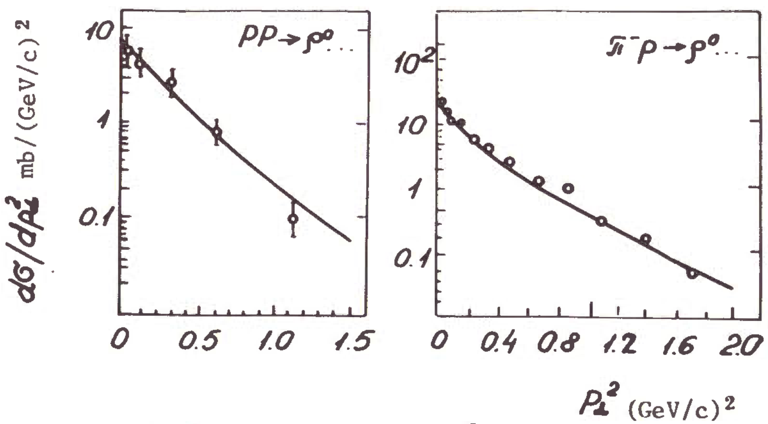

Fig. 9. Distribution of $d\sigma/dp_\perp^2$ for ρ^o-mesons in p-p collisions at T = 11 GeV and π^--p collisions at 15 GeV. The points correspond to experimental data /9–11/.

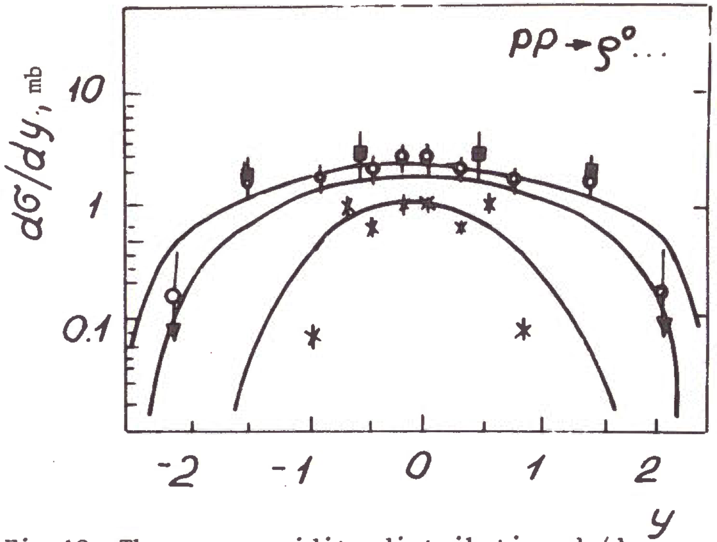

Fig.10. The c.m. rapidity distribution $d\sigma/dy$ ($y = \frac{1}{2}\ln\frac{E+p_\parallel}{E-p_\parallel}$) for ρ^o-mesons in p-p collisions at T = 11 (x), 68 (o) and 200 (■) Gev. Experimental points are taken from /9/.

lastic p-p and π-p collisions. The corresponding angular distributions are shown in Fig.3. As one can see, the majority of the Δ^{++}-resonance have kinetic energy $\mathcal{T} > 0.2\mathcal{T}_{max}$ and are emitted at a narrow angle to the direction of the primary particles*. Distributions for Δ^+- and Δ^o-particles are similar. This allows one to make a conclusion that the majority of the Δ-resonances appear to be the leading particles. At the same time the share of the leading particles among the meson resonances is considerably less frequent.

In Fig.4 the distrubutions of the radius of the space region, connected with the production of resonance $\langle\rho(\mathcal{T})\rangle = \hbar/\langle p_\perp(\mathcal{T})\rangle$, are shown, where $\langle p_\perp(\mathcal{T})\rangle$ is average transverse momentum of the

---

*In the case of p-p interaction the data for the forward hemisphere ($\theta \le \pi/2$) are presented. Because of the symmetry of the initial system they coincide with the data for the backward hemisphere. In the case of π-p interaction the Δ-resonance angles are presented with respect to the direction of the proton motion (i.e., in fact π-θ). For the ρ^o-mesons in the π^--p interaction the distributions for the forward and the backward hemispheres are separately shown in Fig.3 /4/. Within the accuracy of the approximation they are not distinguishable.

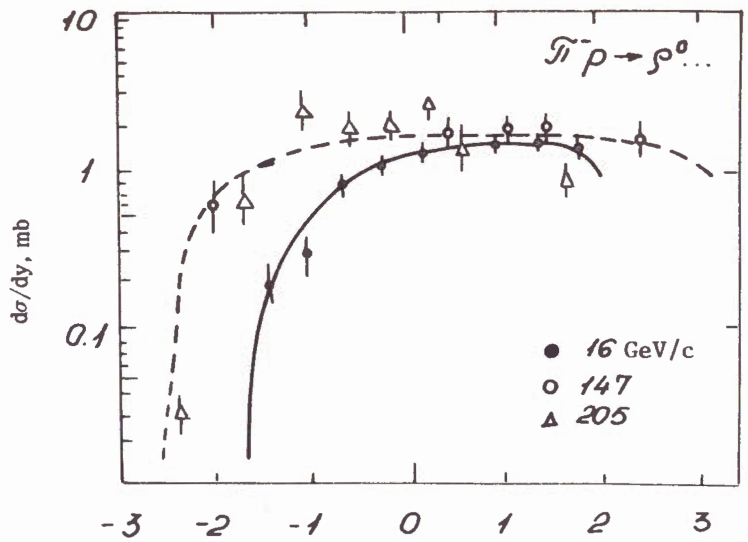

Fig.11. The same as in Fig.10. The inelastic π^--p interaction. The curves are the results of calculations at T = 15 and 200 GeV. The points correspond to experimental data from /9/.

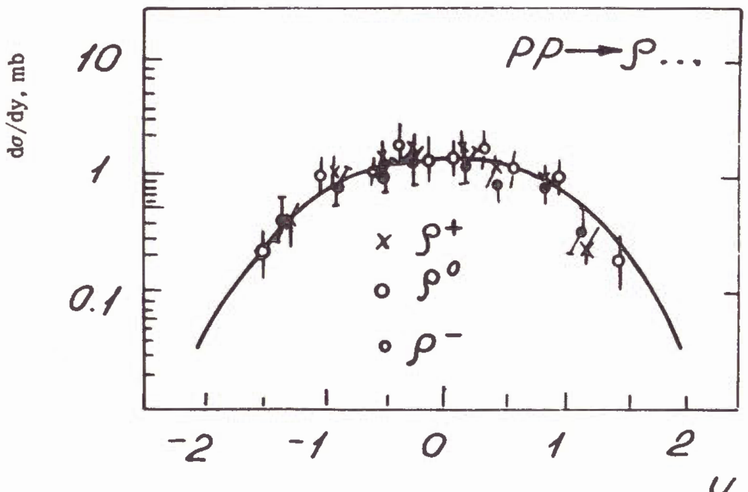

Fig.12. The same as in Fig.10 for ρ^+, ρ^-, and ρ^0-mesons in p-p collisions at T = = 23 GeV /6,23/. The curve is calculated by the expressions (2).

particle of energy T. Comparing these results with the data for nucleons and π-mesons obtained from paper /4/ one can conclude, that high energy barions are produced mainly at big radii. High energy mesons in N-N interaction are produced mainly in a region of smaller radii. In π-N interaction, where the share of the leading mesons is considerably higher, their production is connected with periphery as a rule.

The range of differential distribution approximations of Δ^{++}-resonance is illustrated by Figs.5-7. As in the case of integral characteristics, approximations are in good agreement with the experimental data. In Figs.8-12 we compare with the experiment the various differencial characteristics of ρ^0-mesons, calculated by expressions (1) and (2). The calculations appear to be in good agreement with the experimental data. As for the other charge sign, only fragmentary experimental data are known (see, for example, Fig.12). On the whole, because of the absence of precise fit of the coefficients, agreement of theoretical calculations with the experiment is not so good.

The authors are thankful to Prof.M.G.Mescheryakov for useful discussions and for critical remarks.

REFERENCES

1. Barashenkov V.S., Slavin N.V. Acta Phys.Pol., 1981, B12, No.6, p.563.
2. Barashenkov V.S., Slavin N.V. Acta Phys.Pol., 1981, B12, No.10, p.951.
3. Barashenkov V.S., Slavin N.V. Acta Phys.Pol., 1981, B12, No.10, p.959.
4. Barashenkov V.S., Slavin N.V. Acta Phys.Pol., 1983, B14, No.2, p.89.
5. Slavin N.V. JINR, B1-2-82-744, Dubna, 1982.
6. Grishin V.G. Inclusive Processes in Hadron Interaction at High Energies, Energoizdat, M., 1982.
7. Ammosov V.V. et al. Preprint IHEP, M-19, Serpukhov, 1975; Yad.Fiz., 1976, 24, p.59.
8. Bartke J.et al. Nucl.Phys., 1978, B137, No.3, p.189.
9. Böckmann K. In: Processes of Multiparticle Production and Inclusive Reactions at High Energies, Serpukhov, 1977.
10. Böckmann K. et al. Nucl.Phys., 1980, B166, No.2, p.278.
11. Karimaki V. et al. Report Univ. of Helsinki, HU-p-189, Helsinki, 1980.
12. Brick et al. Phys.Rev., 1980, D21, p.632.
13. Dao F.T. et al. Phys.Rev.Lett., 1973, 30, p.34.
14. Brick D. et al. Phys.Rev.Lett., 1973, 31, p.488.
15. Barish S.J. et al. Phys.Rev., 1975, D12, p.1260; De Brion J.P. et al. Phys.Rev.Lett., 1975, 34, p.910.

16. Lockman W.L. et al. Proc.of the XVIII Intern.Conf.on High Energy Physics, Tbilisi, 1976, D1,2-10400, Dubna, 1977.
17. Ward D.R. et al. Nucl.Phys., 1978, B141, p.203.
18. Likhoded A.K., Shljapnikov P.V. Usp.Fis.Nauk, 1978, 124, p.3.
19. Blobel V. et al. Phys.Lett., 1974, B48, p.73.
20. Winkelmann F.C. et al. Phys.Lett., 1975, B56, p.101.
21. Deutschmann M. et al. Nucl.Phys., 1976, B103, p.426.
22. Singer R. et al. Phys.Lett., 1976, B60, p.385.
23. Böckmann K. et al. Nucl.Phys., 1978, B140, p.235.
24. Albrow M.G. et al. Nucl.Phys., 1979, B155, No.1, p.39.
25. Higgins P.D. et al. Phys.Rev., 1979, D19, No.1, p.65.
26. Suzuki A. et al. Lett.Nuovo Cim., 1979, No.13, p.449.
27. Kichimi H. et al. Phys.Rev., 1979, D20, No.1, p.37.
28. Suzuki A. et al. KEK Preprint 80-3, 1980.
29. Schouten M. et al. Z.Phys., 1981, C9, p.93.
30. Drijard D. et al. Z.Phys., 1981, C9, p.293.
31. Bakken V. et al. Nuovo Cim., 1982, A70, No.2, p.106; 1982, A72, No.4, p.377.
32. Akesson T. et al. Nucl.Phys., 1982, B203, No.1, p.27.
33. Bartke J.et al. Nucl.Phys., 1976, B107, No.1, p.93.
34. Angelov N.S. Proc.of the XVIII Intern.Conf.on High Energy Physics, Tbilisi, 1976, D1,2-10400, Dubna, 1977.
35. Bartle J.et al. Nucl.Phys., 1977, B118, p.360.
36. Grassler H. et al. Nucl.Phys., 1978, B132, p.1.
37. Biswas N.N. et al. Phys.Rev., 1977, D16, p.2090.
38. Schmitz P. et al. Nucl.Phys., 1978, B137, p.13.
39. Brick D. et al. Phys.Rev., 1978, D18, No.9, p.3099.
40. Barreiro F. et al. Phys.Rev., 1978, D17, No.3, p.681.
41. Higgins P.D. et al. Phys.Rev., 1979, D19, p.731.
42. Angelov N.S., Grishin V.G., Kuatadze R.A. Yad.Fiz., 1981, 33, p.1539.

Received by Publishing Department
on April 11, 1984.

SUBJECT CATEGORIES OF THE JINR PUBLICATIONS

Index	Subject
1.	High energy experimental physics
2.	High energy theoretical physics
3.	Low energy experimental physics
4.	Low energy theoretical physics
5.	Mathematics
6.	Nuclear spectroscopy and radiochemistry
7.	Heavy ion physics
8.	Cryogenics
9.	Accelerators
10.	Automatization of data processing
11.	Computing mathematics and technique
12.	Chemistry
13.	Experimental techniques and methods
14.	Solid state physics. Liquids
15.	Experimental physics of nuclear reactions at low energies
16.	Health physics. Shieldings
17.	Theory of condenced matter
18.	Applied researches
19.	Biophysics

Амелин Н.С., Барашенков В.С., Славин Н.В. E2-84-236

Рождение резонансных частиц в неупругих N–N и π–N столкновениях

На основе гипотезы масштабной инвариантности и модели полюсов Редже получены феноменологические выражения для дифференциальных одночастичных сечений образования барионных (Δ^+, Δ°, Δ^{++}) и мезонных ($\rho^\pm$, ρ°, ω) резонансов в неупругих N–N и π–N столкновениях при высоких энергиях. Эти выражения хорошо описывают известные экспериментальных данные в широкой области кинематических переменных примерно от 10 до нескольких тысяч ГэВ. Обсуждаются свойства рождающихся резонансов.

Работа выполнена в Лаборатории вычислительной техники и автоматизации ОИЯИ.

Препринт Объединенного института ядерных исследований. Дубна 1984

Amelin N.S., Barashenkov V.S., Slayin N.V. E2-84-236

Resonance Particle Production in Inelastic N–N and π–N Interactions

Using the considerations connected with the scaling hypothesis and the Regge pole model the phenomenological expressions are obtained for differential single-particle inclusive cross-sections of Δ-, ρ- and ω-resonances in inelastic π–N and N–N collisions at high energies. These expressions describe the known experimental data in a wide energy region from 10 to several thousand GeV.

The investigation has been performed at the Laboratory of Computing Techniques and Automation, JINR.

Preprint of the Joint Institute for Nuclear Research. Dubna 1984